UC Berkeley
UC Berkeley Previously Published Works

Title

Orbital control of the western North Pacific summer monsoon

Permalink

Journal

ISSN

Authors

Wu, Chi-Hua
Chiang, John CH
Hsu, Huang-Hsiung
et al.

Publication Date

DOI

Orbital control of the western North Pacific summer monsoon

Chi-Hua Wu[1] · **John C. H. Chiang**[1,2] · **Huang-Hsiung Hsu**[1] · **Shih-Yu Lee**[1]

space**Abstract** Orbital forcing exerts a strong influence on global monsoon systems, with higher summer insolation leading to stronger summer monsoons in the Northern Hemisphere. However, the associated regional and sea- sonal changes, particularly the interaction between regional monsoon systems, remain unclear. Simulations using the Community Earth System Model demonstrate that the western North Pacific (WNP) summer monsoon responds to orbital forcing opposite to that of other major Northern Hemisphere monsoon systems. Compared with its current climate state, the simulated WNP monsoon and associated lower-tropospheric trough is absent in the early Holocene when the precession-modulated Northern Hemisphere summer insolation is higher, whereas the summer mon- soons in South and East Asia are stronger and shift farther northward. We attribute the weaker WNP monsoon to the stronger diabatic heating of the summer Asian monsoon— in particular over the southern Tibetan Plateau and Mari- time Continent—that in turn strengthens the North Pacific subtropical high through atmospheric teleconnections. By contrast, the impact of the midlatitude circulation changes on the WNP monsoon is weaker when the solar insola- tion is higher. Prior to the present WNP monsoon onset, the upper-tropospheric East Asian jet stream weakens and shifts northward; the monsoon onset is highly affected by the jet-induced high potential vorticity intrusion. In the

spaceinstance of the extreme perihelion-summer, the WNP mon- soon is suppressed despite a stronger midlatitude precursor than present-day, and the midlatitude circulation response to the enhanced South Asian precipitation is considerable. These conditions indicate internal monsoon interactions of an orbital scale, implying a potential mechanistic control of the WNP monsoon.

Keywords Holocene · Orbital forcing · Paleomonsoon · Precession · Western North Pacific

1 Introduction

Evidence from multiple paleoproxy records and numerical modeling has firmly established that orbital changes on Milankovitch timescales alter the global summer monsoons (Wetherald and Manabe 1975; Kutzbach and Guetter 1986; Weber et al. 2004; Berger et al. 2006; Hsu et al. 2010; Ivanova et al. 2012), exerting a substantial effect on the monsoons in North Africa (Martine 1983; Pokras and Mix 1987; Tuenter et al. 2003), Australia (Wyrwoll et al. 2007), India (Braconnot and Marti 2003), and East Asia (An 2000; Wang et al. 2001). However, important details associated with the changes in monsoon seasonality remain unclear (Wang et al. 2003; Liu et al. 2004; Conroy and Over-peck 2011; Chiang et al. 2014), in particular with specific space

regional responses and the potential interactions between

space⁎ Chi-Hua Wu
    chhwu@ntu.edu.tw; chhwu@gate.sinica.edu.tw

[1] Research Center for Environmental Changes,
    Academia Sinica, 128 Academia Road, Section 2, Nankang, Taipei 115, Taiwan

[2] Department of Geography, University of California, Berkeley, CA, USA

spacevarious monsoon subsystems.

Recent work has focused on understanding the impact of precession on the East and South Asian monsoons (Fleit-mann et al. 2007; Wang et al. 2008; Shi et al. 2012; Liu et al. 2014). This activity has been largely motivated by the introduction of high-resolution paleoclimate records during the Holocene that revealed valuable details on the space

spaceregional and seasonal changes (An et al. 2000; Wang et al. 2001; Braconnot and Marti 2003; Liu et al. 2003; Staub-wasser 2006; Jiang et al. 2013, 2014; Nagashima et al. 2013). The summer monsoons in East and South Asia were stronger and penetrated farther north during the early and mid-Holocene compared to today (An et al. 2000; Liu et al. 2014). As the precession-modulated Northern Hemisphere summer insolation decreased after the early Holocene, the "summer optimum" over East Asia (i.e., the timing of peak Holocene rainfall) shifted southwards from northern China in the early Holocene, to central China in the mid-Holo-cene, and to southern China in the late Holocene (An et al. 2000). Nagashima et al. (2013) furthermore suggested that the path of the westerly jet over East Asia varied over the Holocene, apparently in concert with the spatial–temporal variation in East Asian summer precipitation intensity.

In South Asia, Kutzbach and Guetter (1986) found that summer precipitation increased by 10–20 % during the early- to mid-Holocene, but the increase showed large regional contrasts (proxy record). According to Staubwas-ser (2006), water discharged from the Ganga–Brahmaputra

to the Bay of Bengal and precipitation along coastal Oman suggest that the Holocene monsoon wind from the western Arabian Sea exhibited a long-term decrease from its maximum before the mid-Holocene. In western India, however, rainfall increased during the late Holocene, as reflected by an increase in runoff into the eastern Arabian Sea from the Western Ghats (Staubwasser et al. 2002; Staubwasser 2006). These records suggest a southward shift of the Holo- cene summer monsoon in South Asia.

By contrast, relatively few studies have examined paleo-monsoon changes in the western North Pacific (WNP). The WNP monsoon is a major component of the modern Asian-Pacific monsoon (Murakami and Matsumoto 1994; Wang and Lin 2002; Wu et al. 2009). The onset of the modern WNP summer monsoon typically occurs in late July, much later than the summer monsoon onsets in East and South Asia. At onset, a deepened lower-tropospheric monsoon trough appears covering the tropical and subtropical WNP. This occurs simultaneously with an abrupt northward shift of the WNP high that also marks the termination of the Meiyu–Baiu rainy season (Suzuki and Hoskins 2009; Chou et al. 2011); with this transition, the East Asia-WNP region enters into a new monsoon phase (Li and Wang 2005; Wu and Chou 2012; Hsu et al. 2014). The WNP high is also climatically important because of its link to tropical cyclones (Holland 1995; Ueda and Yasunari 1996). The impact of precession on the WNP summer monsoon provides a potential avenue for exploring its dynamics; in particular, its influences and relationship to the adjacent East and South Asian monsoons.

Paleoproxy records, although limited, suggest that the WNP monsoon was weaker during the early Holocene.

spacePrevious studies have suggested that the hydroclimate of the western equatorial Pacific region (e.g., northern Borneo, Papua New Guinea, and the southern Philippines) shifted in phase with precessional forcing (Kissel et al. 2010; Tachi- kawa et al. 2011; Carolin et al. 2013; Fraser et al. 2014), with lowest precipitation during Northern Hemisphere insolation maximum and vice versa.

In this study, we use model simulations to investigate how the seasonal evolution of the WNP summer monsoon is altered under the influence of the precessional cycle. Unlike the other Northern Hemisphere monsoons, we show that the simulated WNP summer monsoon weakens when the precession-modulated Northern Hemisphere summer insolation increases. This indicates that the dynamics of the WNP summer monsoon is quite different from these other monsoons, and we examine the underlying causes of this difference. The data, model, and simulation design are described in Sect. 2. Section 3 reviews the current WNP summer monsoon. Section 4 explores the impact of preces- sion on the WNP summer monsoon, and Sect. 5 explores the potential dynamical causes, focusing on the direct response of the monsoon to changing solar insolation as well as the teleconnected influence of neighboring regional monsoons. We conclude with a summary and discussion in Sect. 6.

2 Data, models, and simulation designs

The data used include precipitation from the Global Precipitation Climatology Project (GPCP) (Huffman et al. 2001) from 1997 to 2013 with a temporal resolution of 1 day and a 1° latitude–longitude spatial resolution; and temperature, humidity, and dynamical fields from the National Centers for Environmental Prediction (NCEP) reanalysis (Kalnay et al. 1996) from 1979 to 2013 with a temporal resolution of 6 h and a 2.5° latitude–longitude spatial resolution.

The atmospheric general circulation model (AGCM) used is the Community Atmospheric Model (CAM) Version 5.1 of the National Center for Atmospheric Research (NCAR), coupled with a slab ocean model (SOM) (http://www.cesm.ucar.edu). Observed present-day heat transports by ocean currents are prescribed on the SOM through a so-called "Q-flux" during the simulation to maintain a simulated sea surface temperature (SST) close to the observed. Boundary and initial conditions are adopted from the Community Earth System Model (CESM) preindustrial control experiment (Vertenstein et al. 2010). Our CAM/SOM simulations are integrated using a finite-volume dynamical core with a standard resolution of 30 vertical levels at a horizontal resolution of approximately 1°. For each simulation case, the model is integrated for 40 years and the outputs for years 21–40 are analyzed. Our analysis of space
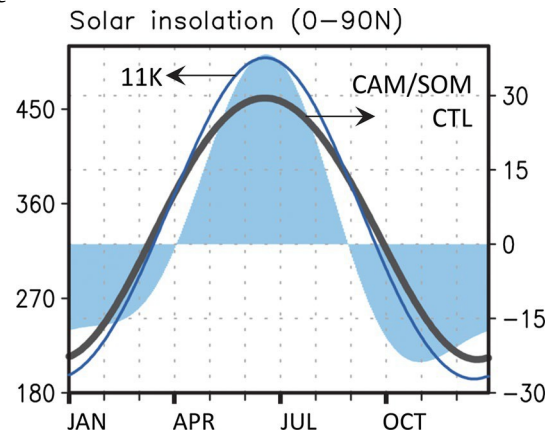

Fig. 1 Annual cycle of solar insolation at the top of the atmosphere in the Northern Hemisphere (0–90°N). *Thick-black* (*thin-blue*) *line* denotes the CAM/SOM present-day (11 K) simulation ranging from 180 to 500 W m^{-2}, and *shadings* denote the 11K simulation minus control simulation (right side coordinate)

model transients indicate that 20 years is sufficient for the model to reach a quasi-equilibrium state; this is consistent with other AGCMs when coupled with SOM (Kitoh 2002; Danabasoglu and Gent 2009).

The CAM/SOM control simulation is conducted with the present-day orbital conditions. The early Holocene simulation (hereafter the '11K simulation') uses orbital conditions 11,000 years before the present day (11 ka BP); the changes to the orbit are primarily from its precessional component; the other boundary conditions are kept the same as present-day conditions. In the Northern Hemisphere, the summer solar insolation in 11 ka BP is much higher than the present-day value (Fig. 1). However, the comparison between paleodata and our 11K simulation is limited to the extent that the imposition of present-day land-surface conditions and greenhouse forcings affects the simulation.

We also use a simplified global climate model (Simplified Parameterizations, privitivE-Equation Dynamics, SPEEDY) to investigate the responses of circulation to regional diabatic heating and distinct solar insolation. The 8-layer SPEEDY, developed at the International Centre for Theoretical Physics (ICTP), has relatively simplified physi- cal parameterizations implemented with a relatively coarse 3.75° longitude–latitude resolution (Molteni 2003; Kuchar- ski et al. 2006); it is also coupled to a SOM. It is computa- tionally lightweight and allows for longer integrations and more cases.

SPEEDY simulation is 100 year 71–100 are analyzed. Despite i is able to simulate the major cir Asia-WNP sector, particularly and the WNP high.

3 spacePresent-day weste summer monsoon

The evolution of the lower signifi- cantly affects the summ and East Asia. The late-July associated deepening of the mo rapid north- ward shift of the W zonally-elon- gated meridic associated with this onset, som Japan (PJ) pattern, is an intrins 1987; Kosaka and Naka- mura the East Asia-WNP region, ther in the monsoon evolution elsew 2c); as such, the mechanis- tic monsoon with the adjacent mc the Indian and Australian mons likely insignificant. The effecti in simulating the present-day I transition is readily obser comparison with the reanalysis

The march of present monso and the WNP high in early sum to the WNP monsoon onset in almost stationary in time (the is located near Taiwan around

appears to follow the progression of the entire Asian monsoon system. By the middle of June, the column-integrated atmospheric heating over the Tibetan Plateau reaches its highest value (Fig. 3a). The South Asian summer monsoon enters its mature phase (as indicated by the strength of the 200-hPa geopotential height shown in Fig. 3a), and the period also corresponds to the onset of the Meiyu–Baiu season over East Asia (Fig. 4a). The center of the upper-tropospheric high over Asia is also relatively stationary in the period prior to the WNP monsoon onset, around 27°N–30°N over the southern Tibetan Plateau (Fig. 3a). The meridional position of this high coincides with the location of the Meiyu–Baiu rain band, implying that the regulation of the present monsoons in South Asia and East Asia and the WNP high is potentially related in the early summer.

Prior to the WNP monsoon onset, the surface wester-lies are weak and the cloud amount is small because of the strong WNP high. Consequently, the heating of the ocean is strong and this increasing SST has been suggested to favor the sudden northward shift of convection from the Philip- pine Sea during the WNP monsoon onset (Ueda et al. 1995; Wu 2002). Nevertheless, the atmosphere is stable,
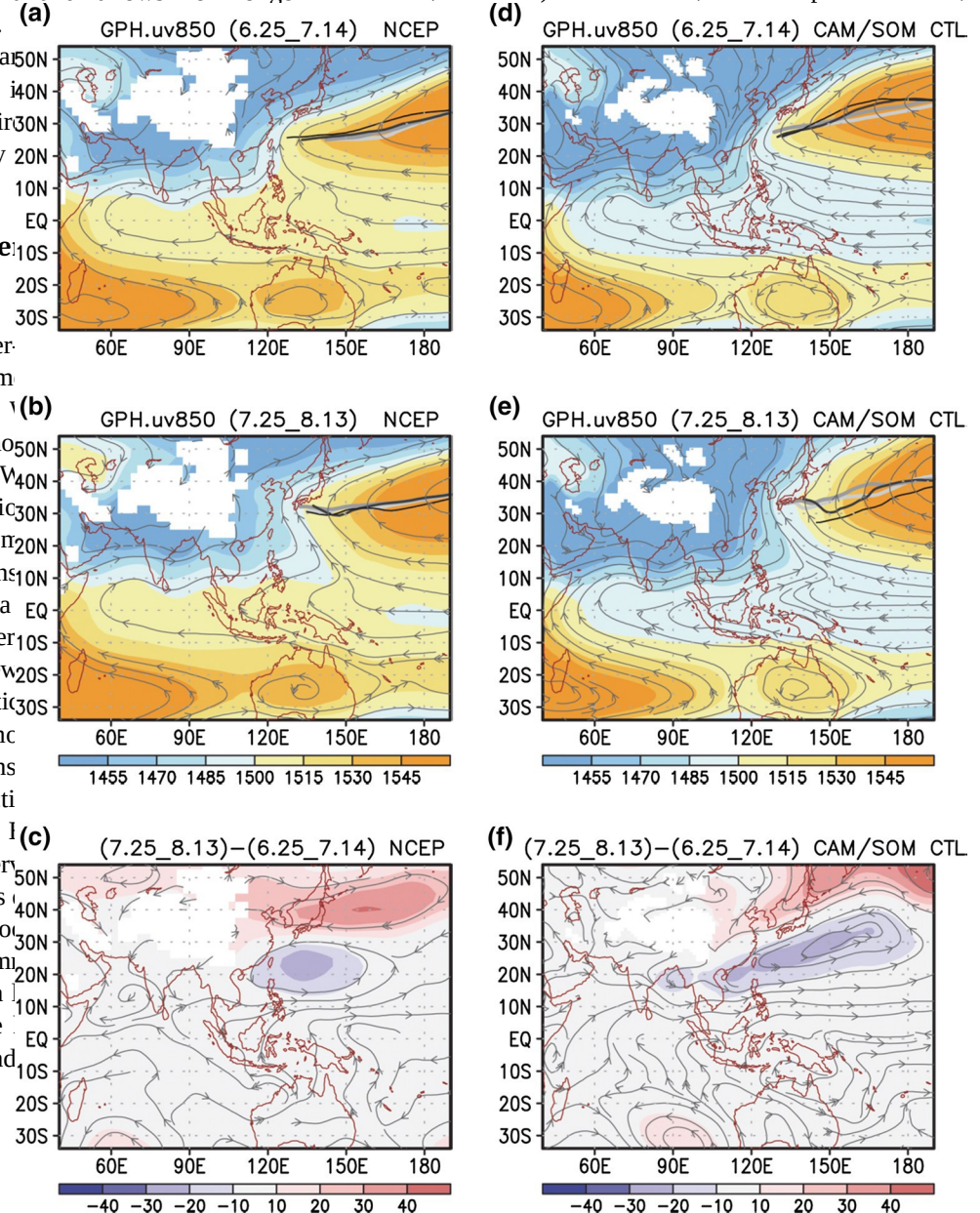
) and streamlines at the 850 hPa of **a** 25 June–14 July, **b** 25 July–13 August and **c** 25 July–13 August minus 25 June–14 July (data from the

NCEP reanalysis). *Black and gray lines* denote evolution of pentad mean geopotential height ridges in the period. **d–f** Same as **a–c** exce

pt for CAM/SOM control simulation

space

Ueda et al. 2009; Suzuki and Hoskins 2009). In general, the onset monsoons over South and Southeast Asia (including the WNP monsoon) have a stepwise character, and there is a general eastward progression in its occurrence. The step-wise monsoon onset is primarily attributed to the air–sea interaction (Wu 2002) as well as seasonal phase-locked intraseasonal oscillation (Wu and Wang 2001).

A number of studies have also suggested that midlati-tude planetary waves resulting from continental heating is responsible for the monsoon transition over the East Asia-WNP region (Sato et al. 2005; Wu et al. 2009; Wu and Chou 2012). Suzuki and Hoskins (2009) suggest that an equivalent barotropic Rossby wave-train developing downstream across Eurasia terminates the Baiu season. Wu and Chou (2012)

space

examine the interannual variability in the WNP monsoon onset from 1974 to 2010, concluding that remote forcing is responsible for rapid intensification of convection during the WNP monsoon onset. They find that, prior to the rapid transi- tion, the northeastern stretch of the South Asian high as well as the upper-tropospheric East Asian jet stream weakens, upper-level divergence in the region southwest of the mid- North Pacific trough increases, and convection is enhanced. In concert with a southward and westward intrusion of the upper-level high potential vorticity (PV), convection expands from the midocean region westward to cover the entire sub- tropical WNP (e.g., 130°E–150°E shown in Fig. 4a).

In brief, the present-day WNP monsoon onset can be pri-marily attributed to a strong extratropical-tropical interaction.
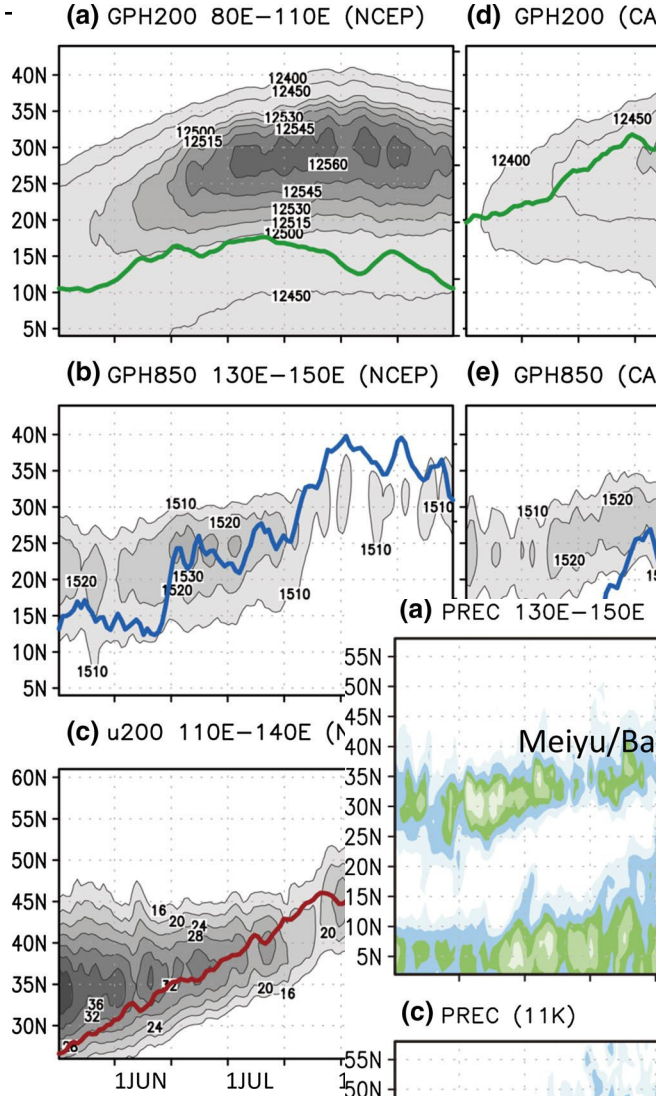
space

(a) GPH200 80E–110E (NCEP)

(d) GPH200 (CA

(b) GPH850 130E–150E (NCEP)
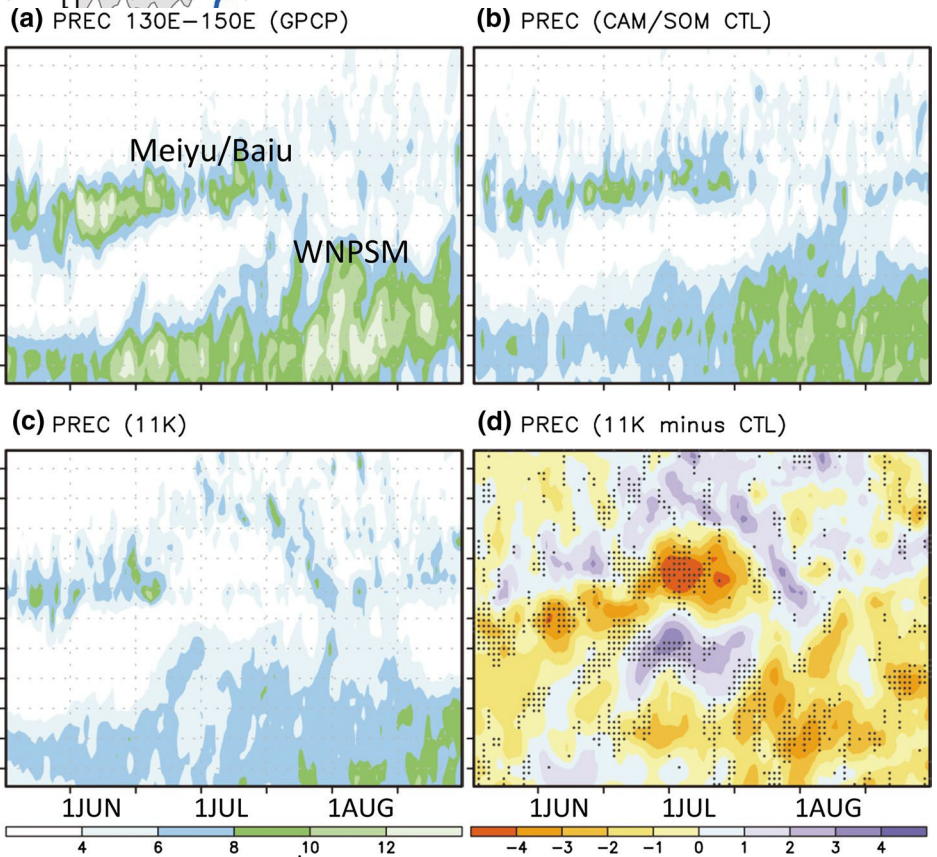
(e) GPH850 (CA

(c) u200 110E–140E (N

Asian monsoon and the corresponding strengthened WNP high suppress the WNP monsoon; and (2) the extratropical influence on the WNP climate weakens after the land–sea thermal contrast becomes dominant.

4 spacePrecessional forcing on the western North Pacific summer monsoon

4.1 Modulation of seasonality

In the 11K simulation, the upper-tropospheric high over South Asia (Fig. 3g) and the lower-tropospheric high over the WNP (Fig. 3h) strengthen considerably relative to the present-day, in particular during July. This indicates a substantial change in the large-scale controls of the 11K WNP summer monsoon. A measure of the WNP monsoon space

(a) PREC 130E–150E (GPCP) Meiyu/Baiu WNPSM

(b) PREC (CAM/SOM CTL)

(c) PREC (11K)

(d) PREC (11K minus CTL)

space**Fig. 3** Latitude-time cross sec
height (gpm) in 80°E–110°E, **b** 8
130°E–150°E and **c** 200-hPa zonal
140°E from the NCEP reanalysis dat
except they show the results of the
simulations, respec- tively. *Green*
column-integrated total heat- ing (W
(higher than 3 km, Hsu and Liu

space2003). *Blue lines* denote
quantified accord- ing to the differenc
s⁻¹) between regions (100°E–130°E,
20°N–30°N) (Wang and

Fan 1999). *Red lines* denote the 200-hPa zonal wind speed (m s⁻¹) in region (110°E–140°E, 30°N–50°N). Right-side coordinates are for the three indices
space

spacePrior to the WNP monsoon onset, the South and East Asian monsoons as well as the WNP high are all at their respective maxima, and relatively stationary; the suggestion is that these monsoon peaks and the peak WNP high are causally related. During early Holocene climate, the monsoons are stronger and shift farther northward in South Asia and East Asia, as a result of the increased summer insolation. We hypothesize that (1) a stronger

ions

of

precipi

tation (mm day^{-1}) averaged over the region (130°E–150°E): **a** observed data, **b** CAM/SOM control simulation, **c** 11K simulation and **d** 11K sim

ulation minus control simulation. *Dots* denote that the precipitation dif-ference has a 99% confidence level

strength (as shown by the blue line of Fig. 3h) reflects weaker monsoon conditions during 11K, presumably due to the dominance of an anticyclonic ridge

with a prevail- ing easterly wind in the south (Fig. 3h). The East Asian jet stream weakens considerably in June; its wind speed drops to almost zero in early July (Fig. 3i). We infer that the land–sea thermal contrast induced by stronger 11K North- ern Hemisphere summer solar heating forces a continental- low and oceanic-high stationary wave pattern.

Figure 4 shows the precipitation evolution in the East Asia-WNP region in a cross section along the 130°E–150°E longitudinal band. The simulated seasonal changes of precipitation in the control run are reason- ably consistent with the current climatology (compare Fig. 4a with 4b). Along the northern edge of the WNP high (Fig. 3b, e), the Meiyu–Baiu precipitation band is the major feature of the early-summer monsoon in the domain (Fig. 4a, b) until mid-late July, when the major convection region shifts from the Meiyu–Baiu region (30°N–40°N) to the subtropical WNP (5°N–25°N) (Ueda et al. 1995) and the WNP summer monsoon onset occurs. In the 11K simu- lation, precipitation over the subtropical WNP is much weaker than that in the present-day simulation (Fig. 4d) because of the stronger WNP high (Fig. 3h). There is a surge in precipitation in late June over the subtropical

spaceWNP which extends into July (Fig. 4c, d), but this should not be interpreted as an earlier WNP monsoon onset because the monsoon trough is absent.

The earlier break in Meiyu–Baiu precipitation may be attributed to the abrupt development of the WNP high. As shown in Fig. 3h, the WNP high shifts northward and matures in mid-June, a month ahead of that in the present-day simulation. This earlier break is consistent with a proxy record of Japan Sea sediments that shows an early-Holocene environment drier than that in the present day (Nagashima et al. 2013).

4.2 Modulation of the western North Pacific monsoon precursors

Due to the precession-induced stronger summer insola- tion, the surface temperature is higher than present-day levels in most regions especially over the Eurasian conti- nent, and the thermal contrast between the Asian conti- nent and North Pacific is greatly enhanced (Fig. 5c). The enhanced land–sea thermal contrast induces a stronger and northward-shifted continental low over Asian land areas and an enhanced and westward-shifted oceanic subtropi- cal high over the North Pacific (Fig. 5c). Figure 6 shows the vertical distribution of geopotential height and vertical
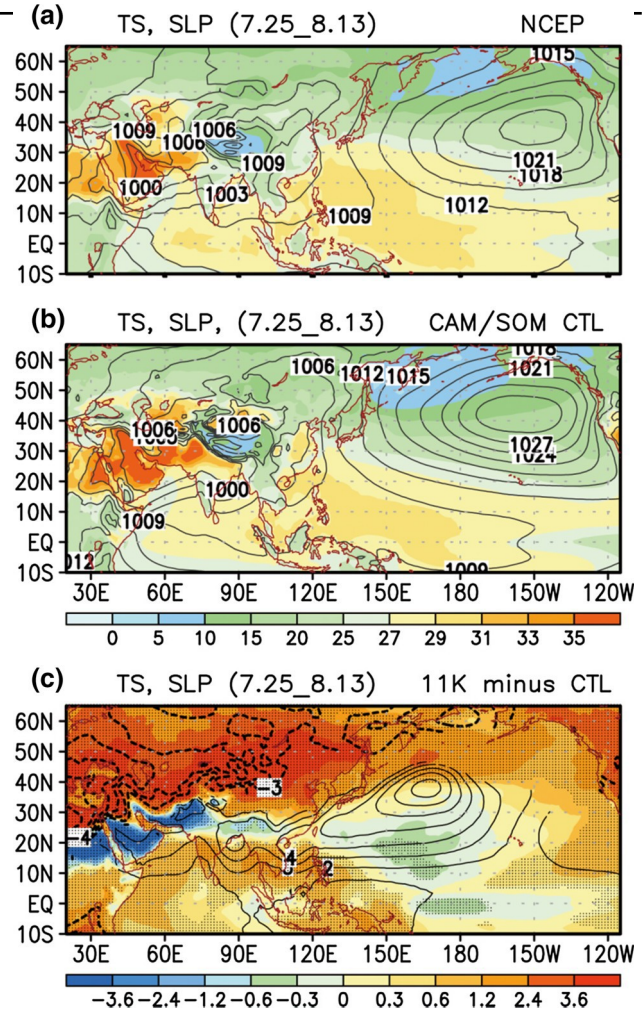
space

Fig. 5 Surface temperature (°C, *shadings*) and sea-level pressure (hPa, *contours*) from 25 July to 13 August: **a** reanalysis data; **b** CAM/ SOM control simulation; **c** 11K simulation minus control simulation. Temperature (sea-level pressure) response with a 99 % confidence level is marked by *dots* (plotted)

air motion along the 20°N–40°N latitudinal band. The geo-potential height in the figure has been subtracted from the zonal average between 20°E and 115°W. Compared with the present-day simulation, the 11K simulation shows a deeper upper-tropospheric trough, stronger lower-tropo- spheric high pressure over the WNP, and an enhanced low pressure over the Asian continent. Correspondingly, both upward motion over East Asia and downward motion over the North Pacific strengthen (Fig. 6c). The upward motion near the East Asian coast is substantially reduced in 11 ka BP because of the westward expansion of the North Pacific high. The atmospheric response to the perihelion-summer solar insolation is consistent with a stronger zonal land–sea thermal contrast.

The stronger land–sea thermal contrast in turn leads to a northward shift of monsoon precipitation in South and
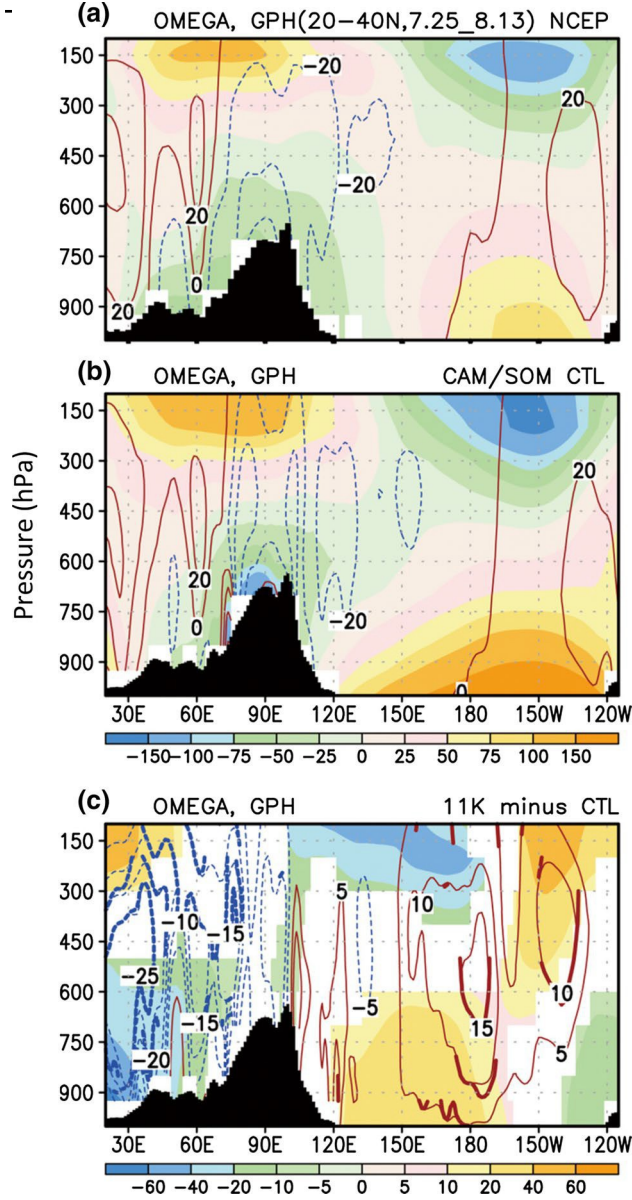
space

Fig. 6 Vertical velocity (hPa day^{-1}, *contours*) and geopotential height (gpm, *shadings*, zonal mean has been subtracted) in the 20°N–40°N longitude–pressure plane from 25 July to 13 August: **a** reanalysis data; **b** CAM/SOM control simulation; **c** 11K simulation minus control simulation. Geopotential height response only with a 99 % confidence level is shown; *thick contours* denote the vertical velocity response with a 99 % confidence level. *Black bars* denote topography

space**Fig. 7 a**–**c** Precipitation (mm day^{-1}, *shadings*), 925-hPa moisture flux (g kg^{-1} m s^{-1}), and 850-hPa geopotential height (gpm, *contours*) and **d**–**f** 200-hPa wind vector, geopotential height (*shadings*), and zonal wind speed (m s^{-1}, *contours*) of CAM/SOM control simula- tion, 11K simulation, and their difference from 25 June to 14 July.

spaceThe difference in lower-level moisture flux and geopotential height and upper-level wind reaching a 99 % confidence level is shown; the difference in precipitation and the 200-hPa geopotential height having a 99 % confidence level is denoted by *dots*
space

East Asia (Figs. 7c, 8c), i.e., more precipitation over the South Asian lands, northern China, and northeastern Asia; less precipitation over the South Asian oceanic areas, the South China Sea, the WNP, central eastern China, and Japan. The overall precipitation changes are consistent with the documented paleo-monsoon characteristics in the early Holocene (An et al. 2000). Similar changes in the North Pacific high and monsoon precipitation in response
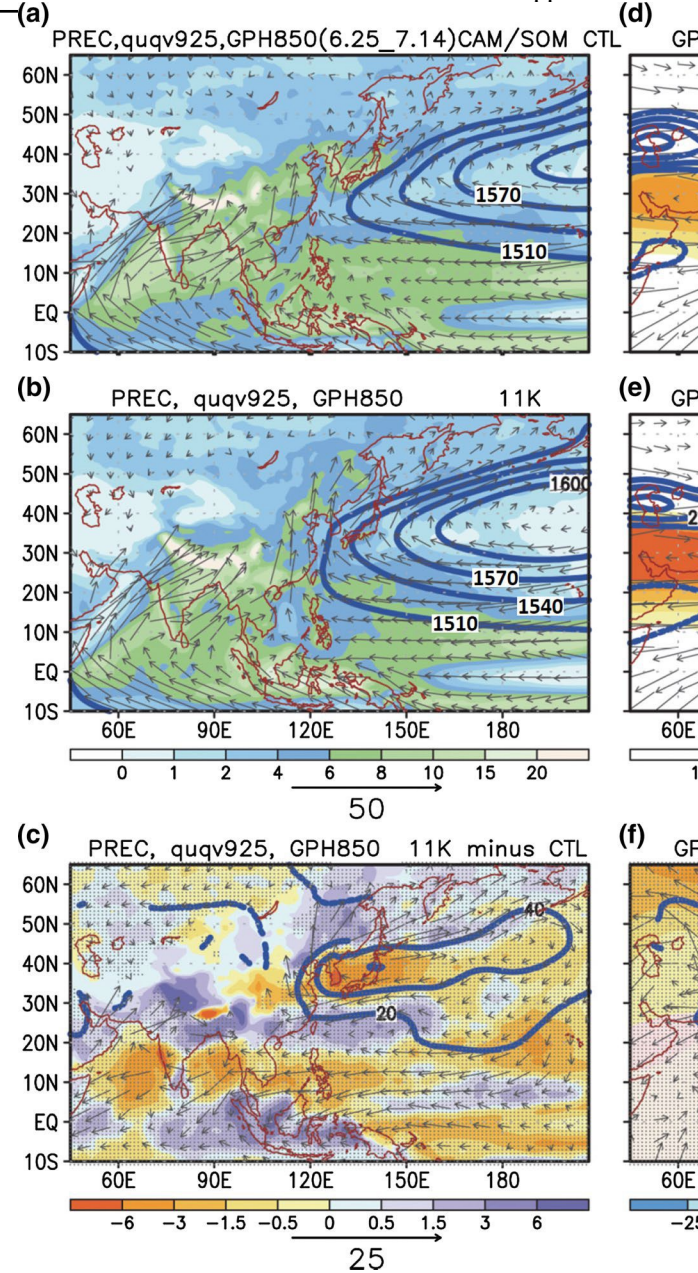space

spaceto precessional forcing are apparent in fully coupled mod- eling studies (Liu et al. 2003; Mantsis et al. 2010, 2013; Jin et al. 2014). We also notice dissimilar precipitation changes among the models over certain areas of East Asia. A number of studies have focused on the topographic effects on the monsoon and suggested that a poorly rep- resented topography might lead to model

biases (Wu et al. 2014 and reference therein); however, it is not well

spaceunderstood how a fine-scale mountain would affect the monsoon circulation.

Wu and Chou (2012) suggested that the extratropical disturbances in the upper troposphere play a crucial role in preconditioning the current late-July monsoon onset over the WNP. This view has been substantially supported by Geng et al. (2014). The extratropical disturbance, which is induced by the weakening of the East Asian jet
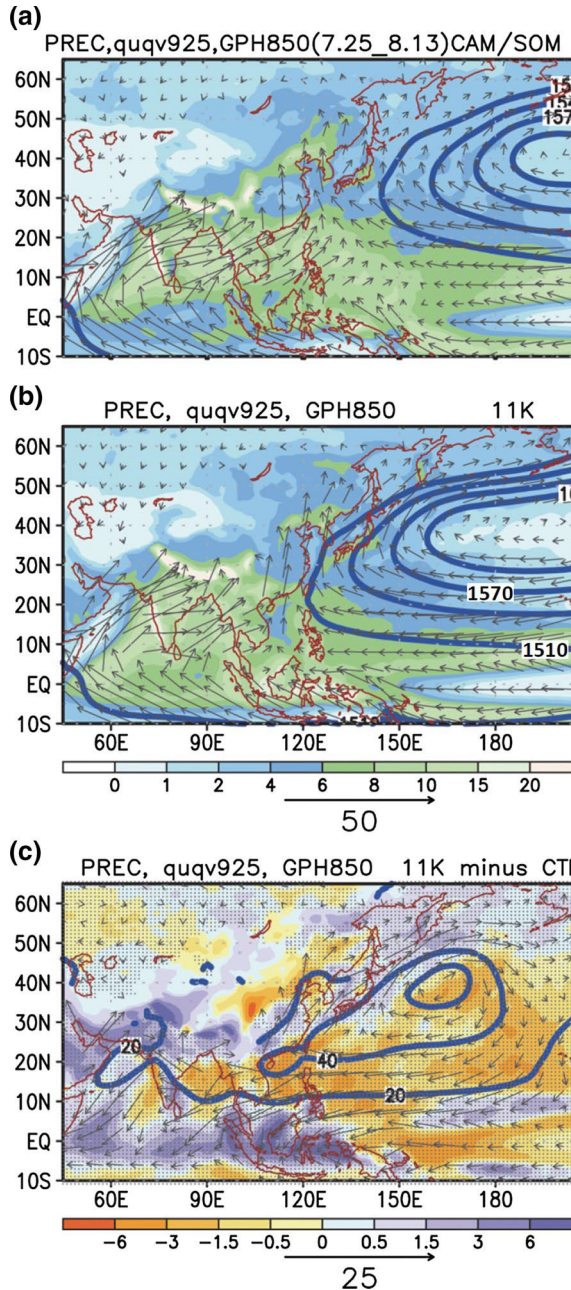
space

Fig. 8 Same as Fig. 7, but shows the results for 25 July to 13 August

spacestream, affects the WNP monsoon by the southward and westward intrusion of upper-level high PV. Prior to the WNP monsoon onset, convection is enhanced over the mid North Pacific associated with the high-PV evolution; the further expansion of the convection triggers the mon- soon onset.

To illustrate the impact of precession on the extratropical disturbances in preconditioning the monsoon, Fig. 7 shows the key thermal and dynamical conditions from 25 June

spaceto 14 July. As noted before, the South and East Asian pre- cipitation in the 11K simulation shifts markedly northward compared with that in the present-day simulation. This shift appears to be a result of a number of factors. First, the monsoonal lower-tropospheric moisture flux increases and penetrates further northwards (Fig. 7c). There is also an increase in the horizontal temperature advection in the midtroposphere into the Meiyu–Baiu region (30°N–40°N, not shown in the figure); Sampe and Xie (2010) argues

space

spacethat this warm advection is a controlling factor in ascend- ing motions (and hence precipitation) in the Meiyu–Baiu region. In the upper troposphere, the East Asian jet stream is weaker, shifts northward, and is confined over the conti- nent; this is consistent with the anticyclonic circulation and high pressure anomaly in East Asia (Fig. 7f).

During 25 June to 14 July, the mid North Pacific upper-level trough is much deeper in the 11K simulation than   in the present-day simulation (compare Fig. 7d with 7e). The deepened upper-level trough, which generally cor- responds to a marked intrusion of high PV air, favors the development of pre-monsoon convection over the ocean. In response to precessional forcing, precipitation is enhanced over the subtropical WNP prior to the WNP monsoon onset, despite the lower-level monsoon trough not being formed. In the present-day climate, enhanced precipita- tion over the subtropical WNP deepens the upper-level trough (Fig. 7c, f), bringing about a positive feedback. The response of PV and vertical motion to the precessional forcing demonstrates the impact of the deepened trough. Along the 20°N–25°N latitudinal band (coinciding with the deepened upper-level trough) the PV is much greater in the 11K simulation than in the present-day simulation (not shown in the figure). Again, the increase in precipitation in this period over the subtropical WNP should not be inter- preted as an earlier WNP monsoon onset because the mon- soon trough is absent.

The stronger WNP high in the 11K simulation that continues into late July and August suppresses the devel- opment of the WNP monsoon trough. From 25 July to 13 August, when the present-day WNP monsoon occurs, there is no monsoon trough over the WNP in the 11K simulation (Fig. 8b). During this period, the South Asian high is much stronger and covers a much larger area (compare Fig. 8d with 8e), and precipitation increases markedly in the south-

ern Tibetan Plateau and North India (Fig. 8a–c). Because of precessional forcing, monsoon heating in South Asia is greatly enhanced after early summer. Over the Tibetan Plateau, atmospheric column-integrated diabatic heating is 35 % (23 %) greater from 25 June to 14 July (25 July to 13 August) in the 11K simulation than in the present-day simulation. The enhancement and northward shift of precipitation in South Asia as well as much higher heating over the Tibetan Plateau plays a crucial role in enhancing the WNP high.

The change seen in 25 June–14 July indicates a much weakened Meiyu–Baiu activity, and the change in 25 July–13 August indicates a much weakened or disappeared WNP summer monsoon. These changes seem to make the sub- seasonal northward march of the East Asia-WNP monsoon phase less apparent. The mid-summer monsoon transition seen in current climate might not be the case 11 ka BP.

5 spaceInterconnection of monsoon subsystems and impact of solar insolation change

5.1 Sensitivity to the monsoon heating of South Asia

Mantsis et al. (2013) simulated the large expansion of the summer anticyclone over the North Pacific during a precessional maximum and suggested that the remote diabatic heating associated with the strengthened summer monsoon in Southeast Asia and Africa could force the WNP high to expand. As shown in Figs. 7c and 8c, precipitation over the Himalayas and North India (60°E–100°E, 20°N–35°N; SA) and the Maritime Continent (90°E–135°E, 5°S–5°N; MC) increases markedly in the 11K simulation.

To test this idea, we investigate the simulated atmospheric response to the diabatic heating in these two regions from July to August using the SPEEDY model. The rea- sonable simulation of the mean July–August climatol- ogy shown in Fig. 9a, b demonstrates the ability of the model in evaluating the influence of anomalous heating. Three extra 100-year simulations are conducted by pre- scribing 0.5 K day^{-1} heating in South Asia and the Mari- time Continent, individually (SA, MC) and also combined (SA MC). The WNP high and upper-level jet stream response in the SPEEDY model to the imposed tropo- spheric heating (SA MC, Fig. 9g, h) is similarly to that seen in our CAM/SOM simulations, in particular an anom- alous anticyclone over the WNP (compare Figs. 8c, 9g) and northeastern Asia (compare Figs. 8f, 9h).

Furthermore, by imposing the heating in different regions (see Fig. 9) we find that (1) the weakened lower-tropospheric westerly winds and reduced rainfall in sub-tropical South Asia between the Arabian Sea and South China Sea result from enhanced heating over the Maritime Continent; (2) the enhanced southerly winds and rainfall over North India and the Bay of Bengal result from locally enhanced heating; and (3) the enhancement of the WNP high can be attributed to both heating changes: northern part by heating anomaly over South Asia, southern part by heating anomaly over the Maritime Continent.

5.2 Monsoon response to changing solar insolation

In consideration of the similar responses of the SPEEDY and CAM/SOM simulations, we continue to explore the monsoon response to changing solar insolation, with the solar constant varying between 331 and 354 W m^{-2} by increments of 3 W m^{-2}. The idea here is to isolate the climate response to increasing insolation during the summertime Northern Hemisphere, similar to what happens during 11K. We acknowledge that the insolation forcing applied here differs from that caused by changes to the precessional
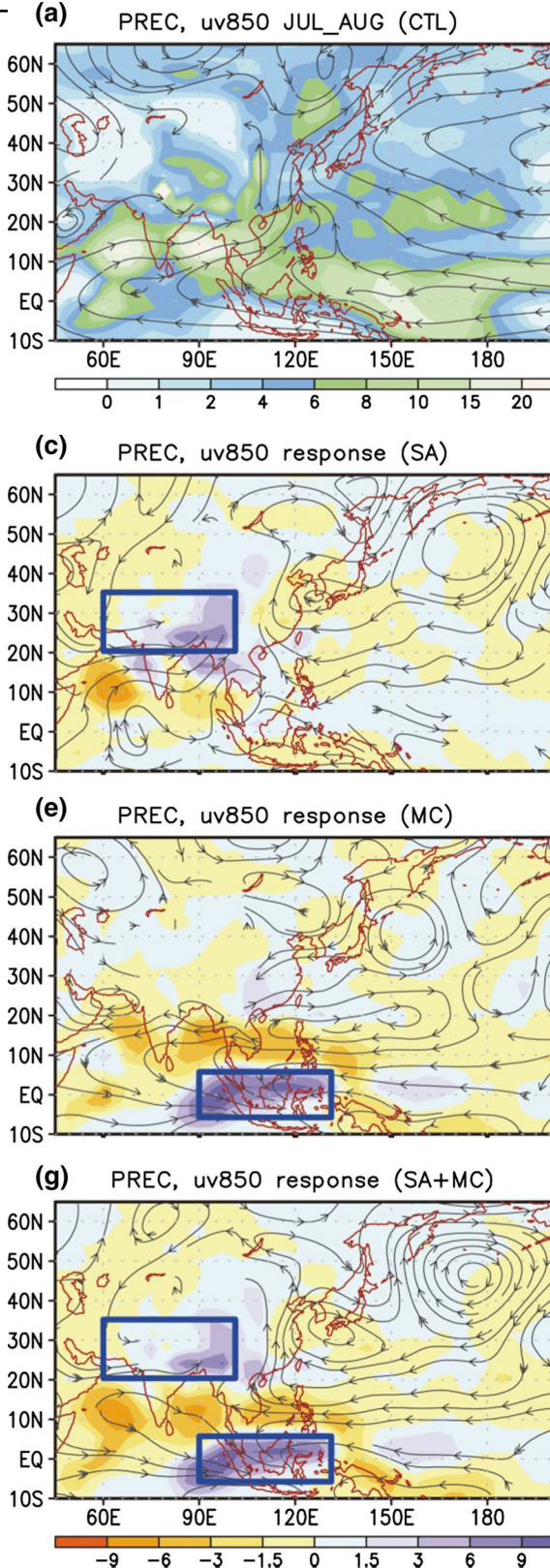
space

(a) PREC, uv850 JUL_AUG (CTL)

space anomalous heating by prescribing 0.5 K day^{-1} heating in South Asia and the Maritime Continent, individually (SA, MC) and also com- bined (SA + MC)
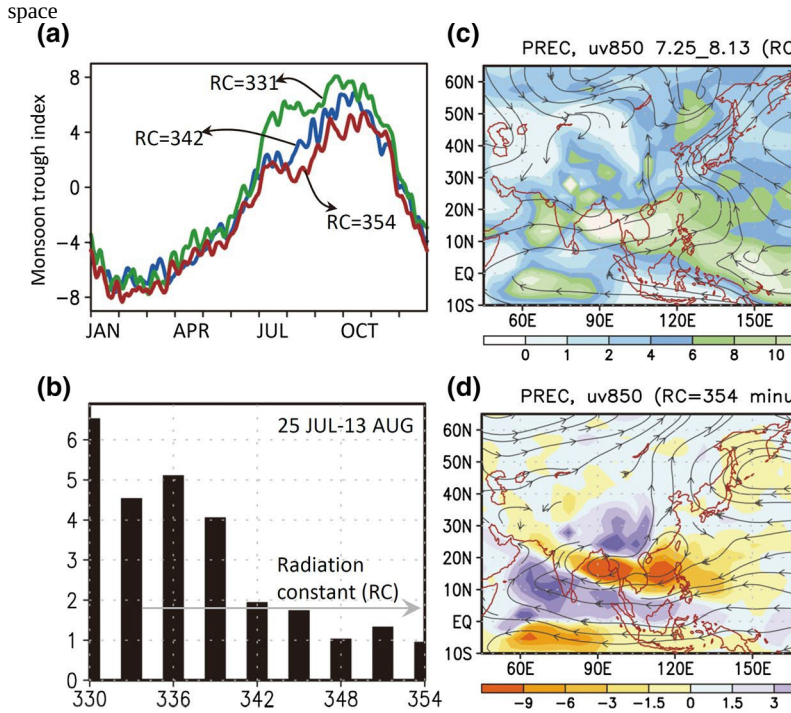
space

(a)

(c) PREC, uv850 7.25_8.13 (RC

(c) PREC, uv850 response (SA)

(b)

(d) PREC, uv850 (RC=354 minu

(e) PREC, uv850 response (MC)

space**Fig. 10 a** Temporal evolution of WNP monsoon index (identi- fied in Fig. 3) of SPEEDY simulations; *green*, *blue* and *red lines* denote the response to radiation constants (RCs) of 331, 342, and 354 W m^{-2}, respectively. **b** Mean WNP monsoon index from 25 July to 13 August in response to the RC between 331 and 354 W m^{-2} in

space increments of 3 W m^{-2}. **c** Precipitation (mm day^{-1}) and 850- hPa streamlines from 25 July to 13 August forced by RC 331 W m^{-2}. **e** Same as **c**, except 200-hPa zonal wind speeds (m s^{-1}) and stream- lines were applied. **d**, **f** Same as **c**, **e**, except the difference between RC = 354 W m^{-2} and RC = 331 W m^{-2}

space

space

(g) PREC, uv850 response (SA+MC)

space**Fig. 9 a** Precipitation (mm day^{-1}) and 850-hPa streamlines and **b** 200-hPa zonal winds and streamlines of SPEEDY control simulation from July to August. **c–h** Same as **a**, **b**, but shows the influence of

cycle in that insolation changes with the latter has sub- stantial latitudinal gradients as well as temporal variation; as such, this may limit the applicability of these idealized simulations to the 11K simulation. One unrealistic setup in our simulations compared to the precession effect is the constant insolation throughout the year. This has the largest potential impact on winter climate. Considering the small bias in insolation caused by this assumption, we assume the impact on the simulation results is minimal. As we will show below, the simulated changes in the summer mon- soons are quite significant. These hypothetic simulations turn out to be informative in understanding the WNP mon- soon response to insolation changes.

Considerable changes in both the strength and timing of onset of the WNP summer monsoon occur as a conse- quence of increasing the solar constant; the WNP mon- soon is stronger and has earlier onsets when the insola- tion is weaker (Fig. 10a). The effect on the WNP monsoon strength from the solar constant changes appears to be largest during July and August. Between 25 July and 13 August, the

change in the strength of the WNP monsoon is not a linear response to the changing insolation. An insola- tion of approximately 342 W m^{-2} (Fig. 10b) seems to be a threshold: the WNP monsoon strengthens considerably

space when the insolation is weaker than 342 W m^{-2}. The poten- tial mechanism is beyond the scope of this study, but will be explored in a future study.

The spatial changes associated with the WNP summer monsoon response to solar constants of 331 and 354 W m^{-2} are shown in Fig. 10c–f. The WNP monsoon trough and upper-level jet stream are much weaker (the monsoon trough only occurrs near 125°E) in the 354 W m^{-2} simula- tion than in the 331 W m^{-2} simulation. Similar to the pre- cessional response in the CAM/SOM simulation (Fig. 8c), precipitation in the 354 W m^{-2} simulation is reduced in response to the prevailing anticyclonic anomaly over the Bay of Bengal, South China Sea, and the WNP, but is enhanced to both north and south over the southern Tibetan Plateau and the tropical northern Indian Ocean (Fig. 10c, d). Correspondingly, the East Asian jet stream and tropical easterly are weaker (Fig. 10e, f). By contrast, the lower- tropospheric westerly is stronger in response to a decrease in solar insolation over the Indochina Peninsula, South China Sea, and the Philippine Sea; this observation is con- sistent with the presence of a deeper WNP monsoon trough and more precipitation over the region.

Thus, the SPEEDY result suggests—at least qualita- tively—that the WNP summer monsoon is suppressed

space

Fig. 11 Schematic diagram of the atmospheric response to the 11 ka BP solar forcing (*light colors and dashed contours*) from 25 July to 13 August. Compared with present-day conditions (*dark colors and solid contours*), the precession-enhanced land–sea thermal contrast results in much stronger upper-tropospheric South Asian high and lower-tropospheric North Pacific high. The upper-level jet stream

spaceweakens, shifts farther north, and is confined over the Asian continent (*blue contours* denote zonal wind speeds, m s^{-1}); and precipitation in South Asia and East Asia markedly shifts

northward relative to its current location (*light blue s̶ ̶ ̶ ̶ ̶ ̶ ̶dings* denote area where precipitation is enhanced). The upper-level Pacific trough is deeper, corresponding to the weaker upper-level jet stream
space

spacebecause of the direct effect of increased summertime Northern Hemisphere solar insolation. The question regard- ing the sensitivity of the WNP summer monsoon to insola- tion changes warrants further study, but is not done here.

6 Concluding remarks and discussion

A CAM/SOM simulation with 11 ka BP orbital forcing is conducted to investigate the impact of precessional changes on the WNP summer monsoon. Our key finding is that unlike the other Northern Hemisphere monsoon systems that increase in intensity when peak Northern Hemisphere summer insolation increases, the WNP summer monsoon actually weakens to the point where the WNP monsoon trough disappears. The reason for the weaker WNP mon- soon is because the WNP high strengthens, which in turn has an adverse effect on the WNP summer monsoon. The WNP high strengthens as a consequence of the enhanced land–sea contrast between the Eurasian continent and the North Pacific. In addition, the increased diabatic heating over the southern Tibetan Plateau and the Maritime Con- tinent also contribute to enhance the WNP high. These changes indicate an interconnection between the Asian-Pacific monsoon subsystems regarding orbital forcing; a strong South Asian summer monsoon may have had an effect on the weakening of the WNP summer monsoon. We used idealized simulations with the SPEEDY model to test the linkages proposed here, and the results support this finding. Besides, we also find that the extratropical

spaceinfluence on the WNP climate weakens after the land–sea thermal contrast becomes dominant.

Figure 11 summarizes the atmospheric responses to pre- cessional change as well as the modulation of the WNP summer monsoon by showing a comparison of the results of the 11K and present-day CAM/SOM simulations. Due to the enhanced land–sea thermal contrast, the upper-trop- ospheric South Asian high and lower-tropospheric North Pacific high is much stronger. The upper-level jet stream weakens, shifts farther north, and is confined over the Asian continent; and precipitation in South Asia and East Asia markedly shifts northward relative to its present-day location. The northward shift of East Asian precipitation is related to the northward shift of the jet stream and expan- sion of the WNP high. Furthermore, the upper-level Pacific trough is deeper, corresponding to the weaker upper-level jet stream; this upper-level circulation change is consistent with the stronger triggering mechanism for the present-day WNP summer-monsoon onset. These atmospheric changes occur despite suppression of the WNP monsoon,
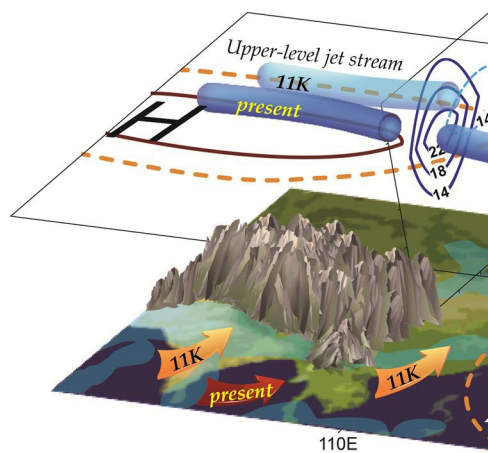
apparently as a consequence of the stronger land–sea thermal contrast as well as the stronger WNP high resulting from enhanced diabatic heating over the southern Tibetan Plateau and the Maritime Continent.

In the 11K simulation, the stronger WNP high and weaker East Asian jet stream similarly occurs in the period prior to the WNP monsoon onset; correspondingly, the Meiyu–Baiu precipitation terminates earlier in late June. The mid-summer monsoon transition seen in present-day climate may not be the case 11 ka BP.

space

space A recent fully-coupled modeling study suggested that El Niño and Southern Oscillation (ENSO)-like forcing substantially affects the monsoon orbital-scale changes in the East Asia-WNP region. Shi et al. (2012) suggested that the precession-scale monsoon variability in East Asia may be influenced by surface cooling over the WNP and surface warming over the eastern tropical Pacific in winter and spring at times of precession maxima. Although a surface-cooling anomaly of the WNP is observed in spring (not shown in the figure) in our CAM/SOM simulation, the SST change is not significant in the eastern tropical Pacific. Internal oceanic feedback could significantly influence the monsoon response to precessional forcing (Caley et al. 2014); this feedback is not accounted for in this study, and warrants further study.

References

An ZS (2000) The history and variability of the East Asian paleomonsoon climate. Quat Sci Rev 19:171–187

An ZS, Porter SC, Kutzbach JE, Wu XH, Wang SM, Liu XD, Li XQ, Zhou WJ (2000) Asynchronous Holocene optimum of the East Asian monsoon. Quat Sci Rev 19:743–762

Berger A, Loutre ME, Mélice JL (2006) Equatorial insolation: from precession harmonics to eccentricity frequencies. Clim Past 2:131–136

Braconnot P, Marti O (2003) Impact of precession on monsoon characteristics from coupled ocean atmosphere experiments: changes in Indian monsoon and Indian ocean climatology. Mar Geol 201:23–34

Caley T, Roche DM, Renssen H (2014) Orbital Asian summer monsoon dynamics revealed using an isotope-enabled global climate model. Nat Commun. doi:10.1038/ncomms6371

Carolin SA, Cobb KM, Adkins JF, Clark B, Conroy JL, Lejau S, Malang J, Tuen AA (2013) Varied response of Western Pacific hydrology to climate forcings over the last glacial period. Science 340:1564–1566

Chiang JCH, Fung IY, Wu CH, Cai YJ, Edman JP, Liu YW, Day JA, Bhattacharya T, Mondal Y, Labrousse CA (2014) Role of seasonal transitions and westerly jets in East Asian paleoclimate. Quat Sci Rev (under revision)

Chou MD, Wu CH, Kau WS (2011) Large-scale control of summer precipitation in Taiwan. J Clim 19:5081–5093

space Conroy JL, Overpeck JT (2011) Regionalization of present-day precipitation in the greater monsoon region of Asia. J Clim 24:4073–4095

Danabasoglu G, Gent PR (2009) Equilibrium climate sensitivity: is it accurate to use a slab ocean model? J Clim 22:2494–2499

Fleitmann D, Burns SJ, Mangini A, Mudelsee M, Kramers J, Villa I, Neff U, Al-Subbary AA, Buettner A, Hippler D, Matter A (2007) Holocene ITCZ and Indian monsoon dynamics recorded in stalagmites from Oman and Yemen (Socotra). Quat Sci Rev 26:170–188

Fraser N, Kuhnt W, Holbourn A, Bolliet T, Andersen N, Blanz T, Beaufort L (2014) Precipitation variability within the West Pacific Warm Pool over the past 120 ka: evidence from the Davao Gulf, southern Philippines. Paleoceanography. doi:10.1002/2013PA002559

Geng B, Yoneyama K, Shirooka R (2014) Observations of upper-trop- ospheric influence on a monsoon trough over the western North Pacific. Mon Weather Rev 142:1472–1488

Holland GJ (1995) Scale interaction in the western Pacific monsoon. Meteorol Atmos Phys 56:57–79

Hsu HH, Liu X (2003) Relationship between the Tibetan Plateau heat- ing and East Asian summer monsoon rainfall. Geophys Res Lett 30:2066–2069

Hsu YH, Chou C, Wei KY (2010) Land–ocean asymmetry of tropical precipitation changes in the mid-Holocene. J Clim 23:4133–4151

Hsu HH, Zhou T, Matsumoto J (2014) East Asian, Indochina and western North Pacific Summer Monsoon: an update. Asia Pac J Atmos Sci 50:45–68

Huffman GJ, Adler RF, Morrissey M, Bolvin DT, Curtis S, Joyce R, McGavock B, Susskind J (2001) Global precipitation at one-degree daily resolution from multi-satellite observations. J Hydrometeor 2:36–50

Ivanova EV, Beaufort L, Vidal L, Kucera M (2012) Precession forcing of productivity in the eastern Equatorial Pacific during the last glacial cycle. Quat Sci Rev 40:64–77

Jiang Z, Ren W, Liu Z, Yang H (2013) Analysis of water vapor transport characteristics during Meiyu over the Yangtze-Huaihe River valley using the Lagrangian method. Acta Meteorol Sin 71:295–304

Jiang X, He Y, Shen CC, Lee SY, Yang B, Lin K, Li Z (2014) Decoupling of the East Asian summer monsoon and Indian summer monsoon between 20 and 17 ka. Quat Res 82:146–153

Jin L, Schneider B, Park W, Latif M, Khon V, Zhang X (2014) The spatial-temporal patterns of Asian summer monsoon precipitation in response to Holocene insolation change: a model-data synthesis. Quat Sci Rev 85:47–62

Kalnay E et al (1996) The NCEP/NCAR 40-year reanalysis project. Bull Am Meteorol Soc 77:437–471

Kissel C, Laj C, Kienast M, Bolliet T, Holbourn A, Hill P, Kuhnt W, Braconnot P (2010) Monsoon variability and deep oceanic circulation in the western equatorial Pacific over the last climatic cycle: insights from sedimentary magnetic properties and sortable silt. Paleoceanography. doi:10.1029/2010PA001980

Kitoh A (2002) Effects of large-scale mountains on surface climate: a coupled ocean–atmosphere general circulation model study. J Meteorol Soc Jpn 80:1165–1181

Kosaka Y, Nakamura H (2006) Structure and dynamics of the summertime Pacific-Japan teleconnection pattern. Q J R Meteorol Soc 132:2009–2030

Kosaka Y, Nakamura H (2010) Mechanisms of meridional teleconnection observed between a summer monsoon system and a subtropical anticyclone. Part I: the Pacific-Japan pattern. J Clim 23:5085–5108

Kucharski F, Molteni F, Bracco A (2006) Decadal interactions between the western tropical Pacific and the North Atlantic Oscillation. Clim Dyn 26:79–91

space

    spaceKutzbach JE, Guetter PJ (1986) The influence of changing orbital parameters and surface boundary conditions on climate simulations for the past 18000 years. J Atmos Sci 15:1726–1759

Li T, Wang B (2005) A review on the western North Pacific summer monsoon: synoptic-to-interannual variabilities. Terr Atmos Ocean Sci 16:285–314

Liu Z, Otto-Bliesner B, Kutzbach J, Li L, Shields C (2003) Coupled climate simulations of the evolution of global monsoons in the Holocene. J Clim 16:2472–2490

Liu Z, Harrison S, Kutzbach J, Otto-Bliesner B (2004) Global monsoons in the mid-Holocene and oceanic feedback. Clim Dyn 22:157–182

Liu Z, Wen X, Brady EC, Otto-Bliesner B, Yu G, Lu H, Cheng H, Wang Y, Zheng W, Ding Y, Edwards RL, Cheng J, Liu W, Yang H (2014) Chinese cave records and the East Asia summer monsoon. Quat Sci Rev 83:115–128

Mantsis DF, Clement AC, Broccoli AJ, Erb MP (2010) Climate feedbacks in response to changes in obliquity. J Clim 24:2830–2845

Mantsis DF, Clement AC, Kirtman B, Broccoli AJ, Erb MP (2013) Precessional cycles and their influence on the North Pacific and North Atlantic summer anticyclones. J Clim 26:4596–4611

Martine RS (1983) African monsoons, an immediate climate response to orbital insolation. Nature 304:46–49

Molteni F (2003) Atmospheric simulations using a GCM with simplified physical parametrizations. I. Model climatology and variability in multi-decadal experiments. Clim Dyn 20:175–191

Murakami T, Matsumoto J (1994) Summer monsoon over the Asian continent and western North Pacific. J Meteorol Soc Jpn 72:719–745

Nagashima K, Tada R, Toyoda S (2013) Westerly jet-East Asian summer monsoon connection during the Holocene. Geochem Geophys Geosyst 14:5041–5053

Nitta T (1987) Convective activities in the tropical western Pacific and their impact on the Northern Hemisphere summer circulation. J Meteorol Soc Jpn 65:373–390

Pokras EM, Mix AC (1987) Earth's precession cycle and Quaternary climatic change in tropical Africa. Nature 326:486–487

Sampe T, Xie SP (2010) Large-scale dynamics of the Meiyu–Baiu rainband: environmental forcing by the westerly jet. J Clim 23:113–134

Sato N, Sakamoto K, Takahashi M (2005) An air mass with high potential vorticity preceding the formation of the Marcus convergence zone. Geophys Res Lett. doi:10.1029/2005GL023572

Shi Z, Liu X, Cheng X (2012) Anti-phased response of northern and southern East Asian summer precipitation to ENSO modulation of orbital forcing. Quat Sci Rev 40:30–38

Staubwasser M (2006) An overview of Holocene South Asian monsoon records: monsoon domains and regional contrasts. J Geol Soc India 68:433–446

Staubwasser M, Sirocko F, Grootes PM, Erlenkeuser H (2002) South Asian monsoon climate and radiocarbon in the Arabian Sea during Early and Mid Holocene. Paleoceanography. doi:10.1029/2000PA00060

Suzuki S, Hoskins B (2009) The large-scale circulation change at the end of the Baiu season in Japan as seen in ERA40 data. J Meteorol Soc Jpn 87:83–99

spaceTachikawa K, Cartapanis O, Vidal L, Beaufort L, Barlyaeva T, Bard E (2011) The precession phase of hydrological variability in the Western Pacific Warm Pool during the past 400 ka. Quat Sci Rev 30:3716–3727

Tuenter E, Weber SL, Hilgen FJ, Lourens LJ (2003) The response of the African summer monsoon to remote and local forcing due to precession and obliquity. Glob Planet Change 36:219–235

Ueda H, Yasunari T (1996) Maturing process of the summer monsoon over the western North Pacific–A coupled ocean/atmosphere sys-tem. J Meteorol Soc Jpn 74:493–508

Ueda H, Yasunari T, Kawamura R (1995) Abrupt seasonal changes of large-scale convective activity over the western Pacific in the northern summer. J Meteorol Soc Jpn 73:795–809

Ueda H, Ohba M, Xie SP (2009) Important factors for the development of the Asian-Northwest Pacific summer monsoon. J Clim 22:649–668

Vertenstein M, Craig T, Middleton A, Feddema D, Fischer C (2010) CESM1.0.3 user's guide. http://www.cesm.ucar.edu/

Wang B, Fan Z (1999) Choice of South Asian Summer monsoon indices. Bull Am Meteorol Sci 80:629–638

Wang B, Lin H (2002) Rainy season of the Asian-Pacific summer monsoon. J Clim 15:386–398

Wang YJ, Cheng H, Edwards RL, An ZS, Wu JY, Shen CC, Dorale JA (2001) A high-resolution absolute-dated late Pleistocene mon-soon record from Hulu Cave. Science 294:2345–2348

Wang B, Clemens SC, Liu P (2003) Contrasting the Indian and East Asian monsoons: implications on geologic timescales. Mar Geol 201:5–21

Wang YJ, Cheng H, Edwards RL, Kong X, Shao X, Chen S, Wu J, Jiang X, Wang X, An ZS (2008) Millennial- and orbital-scale changes in the East Asian monsoon over the past 224,000 years. Nature 451:1090–1093

Weber SL, Crowley TJ, van der Schrier G (2004) Solar irradiance forcing of centennial climate variability during the Holocene. Clim Dyn 22:539–553

Wetherald RT, Manabe S (1975) The effects of changing the solar constant on the climate of a general circulation model. J Atmos Sci 32:2044–2059

Wu R (2002) Processes for the northeastward advance of the summer monsoon over the western North Pacific. J Meteorol Soc Jpn 80:67–83

Wu CH, Chou MD (2012) Upper-tropospheric forcing on late July monsoon transition in East Asia and the western North Pacific. J Clim 25:3929–3941

Wu R, Wang B (2001) Multi-stage onset of the summer monsoon over the western North Pacific. Clim Dyn 17:277–289

Wu CH, Kau WS, Chou MD (2009) Summer monsoon onset in the subtropical western North Pacific. Geophys Res Lett. doi:10.1029/2009GL040168

Wu CH, Hsu HH, Chou MD (2014) Effect of the Arakan Mountains in the northwestern Indochina Peninsula on the late May Asian monsoon transition. J Geophys Res Atmos 119:10769–10779

Wyrwoll KH, Liu Z, Chen G, Kutzbach JE, Liu X (2007) Sensitivity of the Australian summer monsoon to tilt and precession forcing. Quat Sci Rev 26:3043–3057